RSC Advances

PAPER

View Article Online
View Journal | View Issue

Cite this: *RSC Adv.*, 2023, **13**, 31092

Polyether-based waterborne synergists: effect of polymer topologies on pigment dispersion†

Hansol Kang, ‡[ab] Si Eun Kim,‡[a] Young Il Park, [a] Jin Chul Kim, [a] Ji-Eun Jeong,[a] Hyocheol Jung,[a] Hyosun Lee, [c] Sung Yeon Hwang,*[d] In Woo Cheong, *[b] Sang-Ho Lee *[ae] and Eunyong Seo *[af]

Control of polymer topologies is essential to determine their unique physical properties and potential applications. The polymer topologies can have a critical effect on pigment dispersion owing to their unique architectures; however, studies using polymer topologies on pigment dispersion in aqueous systems are scarce. Thus, this study proposes various topologies of polyether-based waterborne synergists, such as linear, hyperbranched, and branched cyclic structures. Specifically, we applied branched types of polyglycidols (PGs) as a synergist to provide polymer topology-dependent dispersibility for the surface-modification of Red 170 particles through adsorption and steric hindrance. The topology-controlled PG synergists (PGSs) were successfully prepared by post-polymerization modification with phthalimide and benzoyl groups. Particularly, the branched types of PGSs, branched cyclic PGS (*bc*-PGS), and hyperbranched PGS (*hb*-PGS) exhibited improved dispersibility through adsorption on top of the pigment, interaction between dispersant (BYK 190) and pigment, and steric effect. Surprisingly, *hb*-PGS conferred the Red 170 pigment particles with superior storage stability than that of *bc*-PGS despite their similar structural features. This study suggests the widespread potential application of PGSs as waterborne synergists for various dispersion applications.

Received 21st September 2023
Accepted 18th October 2023

DOI: 10.1039/d3ra06427a

rsc.li/rsc-advances

Introduction

Dispersion technologies for organic and inorganic pigments used in various industries such as digital printing, paints, coating, cosmetics, and display have been extensively developed. This is because the dispersibility of pigments in a solution significantly affects optical densities, shape spectral properties, transmittance, and color resolution.[1–5] In particular, the design of a high-performance dispersant system should consider numerous factors such as chemical structure, hydrophile–lipophile balance, molecular weight, and molecular-weight distribution for providing a stable dispersion with uniform particle size.[5–10] Additionally, dispersants have received significant attention in dispersion applications, because they can enhance the dispersing ability and durability upon exposure, facilitating higher stability of pigment dispersions. However, obtaining high efficiency in applications by employing dispersing agents remains challenging because of incomplete dispersion and difficulty in complete particle separation. In addition, these limitations lead to uneven coloring, thereby further limiting the advantage of the fully optimized effect.[11,12] To overcome the challenges associated with dispersants in pigment-based products, modulating pigment aggregation forces is essential to maximize the dispersing effect on pigment performance.

Numerous approaches to design the dispersing ability of dispersants using specific surfactants, functionalized polymers, and mineral oxides have been reported.[13,14] Among them, the use of synergists to reinforce traditional dispersant-based methods has recently become a focus in dispersion systems. Specifically, the use of synergists offers interesting opportunities not only for forming strong adsorption of dispersants on pigment surface but also for stabilizing pigment particles by reducing interparticle flocculation through the steric hindrance effect.[15–19] Many of these synergists have been designed based

[a]*Center for Advanced Specialty Chemicals, Korea Research Institute of Chemical Technology, Ulsan 44412, Republic of Korea. E-mail: slee@krict.re.kr*

[b]*Department of Applied Chemistry, Kyungpook National University (KNU), Daegu 41566, Republic of Korea. E-mail: inwoo@knu.ac.kr*

[c]*Department of Chemistry and Green-Nano Materials Research Center, Kyungpook National University, 80 Daehakro, Buk-gu, Daegu 41566, Republic of Korea*

[d]*Department of Plant & Environmental New Resources and Graduate School of Biotechnology, Kyung Hee University, Gyeonggi-do 17104, Republic of Korea. E-mail: crew75@khu.ac.kr*

[e]*Advanced Materials and Chemical Engineering, University of Science and Technology (UST), Daejeon 34113, Republic of Korea*

[f]*Department of Chemical Engineering, Ulsan College, Ulsan 44610, Republic of Korea. E-mail: eyseo@uc.ac.kr*

† Electronic supplementary information (ESI) available: Experimental details; synthetic procedures and characterization of anchor molecules, analysis of topology-controlled PG-based synergists (PDF). See DOI: https://doi.org/10.1039/d3ra06427a

‡ These authors contributed equally to the work.

on chemical structures similar to the targeted pigment molecules. For example, in a phthalocyanine-based dispersion, the core part in the synergist consists of the phthalocyanine molecular structure to facilitate the adsorption of the synergist on the pigment surface.[16] In addition, the edge side of this synergist modified with functional groups, such as primary amine or carboxylic acid, is effectively utilized in binding to anchoring groups of dispersants *via* strong hydrogen bonding. Moreover, Kelley *et al.* reported that acid-functionalized synergists can maintain a high dispersibility of organic pigment particles even in propylene glycol methyl ether acetate-based eco-friendly solvent systems.[18] Although this synergist-based approach provides an optimized interaction with the targeted pigment and excellent dispersing performance, only a few studies using synergists for the preparation of pigment dispersion in aqueous systems have been reported as a result of the limited modification of pigment-based designed synergists. Moreover, to utilize organic pigments in aqueous systems, the organic synergist should essentially include a hydrophilic part or polar features.[19] This synergist-based dispersing approach for aqueous systems is thus highly challenging because dispersibility *via* various types of dispersants and the corresponding properties, such as storage stability, are effectively controllable through the incorporation of synergists with functionalities for interacting between pigment particles and dispersants.

In the past few decades, the control of polymer topologies for managing their unique functions and physical properties has attracted attention.[20,21] As representative examples, dendrimers and hyperbranched polymers have been investigated owing to their interesting physical properties such as excellent solubility, low solution viscosity, and modified rheological properties, which originate from their branched multifunctional structures compared with linear structures.[22–25] Hawker *et al.* reported the polymeric architectural effects on a TiO_2 dispersion using diverse branched poly(acrylic acid) derivatives in comparison to linear polymers in an aqueous system.[26] In addition, Storey *et al.* demonstrated three types of polyisobutylene succinimide analog dispersants (linear, grafted, and comb type) for carbon black dispersion.[27] Compared with linear dispersants in the organic system, the comb- and grafted-type dispersants exhibited greater affinities for adsorption but decreased

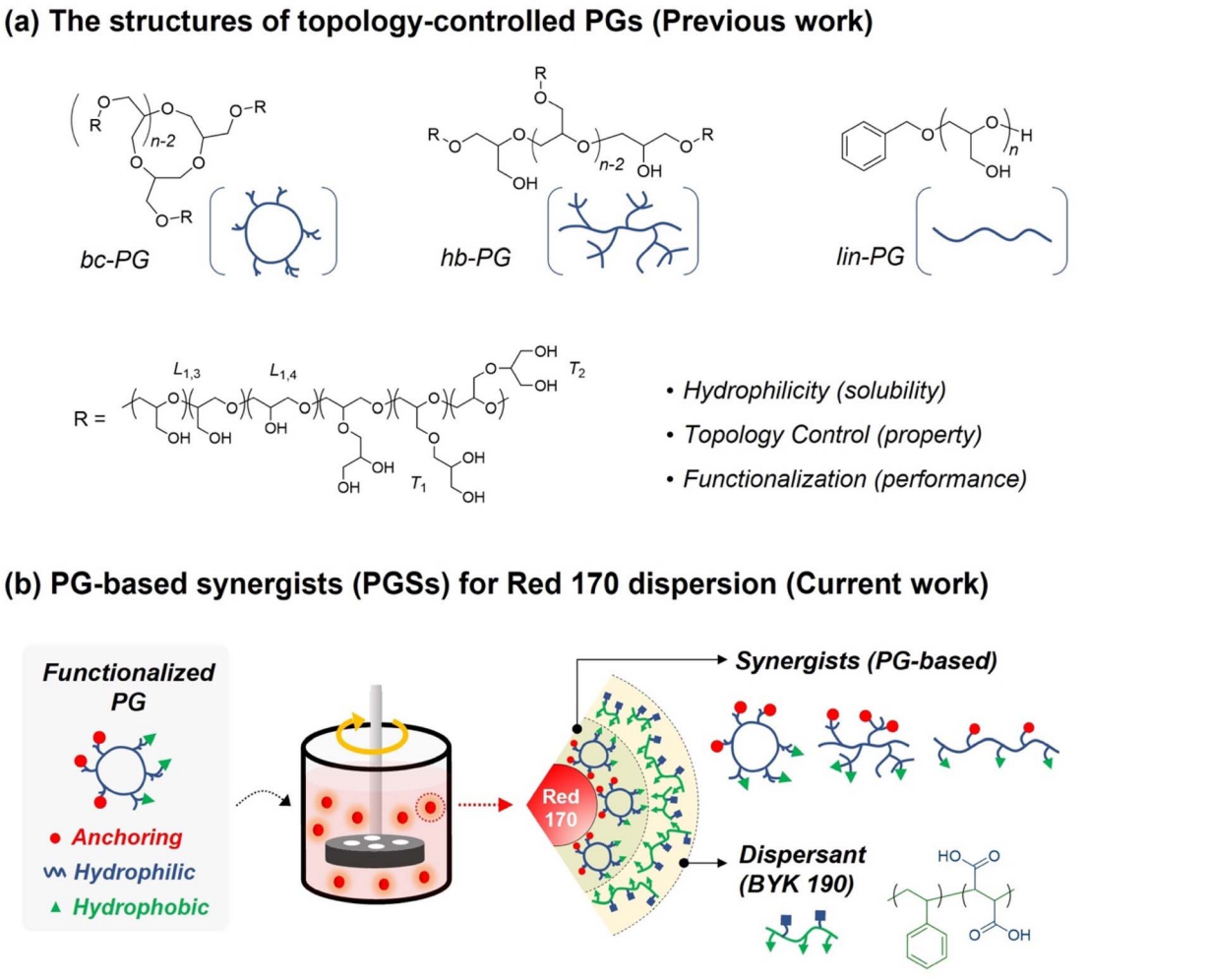

Scheme 1 Research scheme of Red 170 dispersion based on polyether-based synergists. (a) The molecular structure of topology-controlled polyglycidols (PGs), and (b) the pigment dispersion strategy using functionalized PG-based synergists (PGSs) are described in this scheme.

packing efficiencies. Despite the successful improvement of the dispersion performance *via* controlling polymer topologies, most of these investigations have been limited to linear polymer systems;[28–30] thus, we aim to seek further tuning of the dispersion performance *via* precise control of polymeric topology.

In our previous work, hyperbranched polyglycidols (*hb*-PGs) and branched cyclic PGs (*bc*-PGs) were successfully synthesized *via* metal-free ring-opening polymerization of glycidol using frustrated Lewis pairs along with linear PGs (*lin*-PGs) having a similar degree of polymerization (DP_n) as control (Scheme 1a)[31,32] We found that precisely controlled polymer topologies are important factors in determining their unique properties, such as enhanced adhesion performance *via* cooperative hydrogen bonding between polymer chains with excellent biocompatibility and enhanced self-healing efficiency *via* different polymer network mesh space.[33,34] Evidently, a highly flexible polyether backbone with multiple functional hydroxyl groups would be suitable as a polymer-based synergist in aqueous dispersion system because its strong hydrophilic feature can provide organic pigment particles with high aqueous solubility. Additionally, numerous hydroxy groups in pendants can allow for variable functionalization *via* post-polymerization modification, such as the introduction of hydrophobic groups or anchor moieties (Scheme 1b). Herein, we present the potential application of topology-controlled polyglycidol-based waterborne synergists (PGSs) with different anchor groups on dispersion performance. The Red 170 pigment iswidely used in various industries, and BYK 190 as a polymeric dispersant mixed with styrene and maleic acid has been applied to our aqueous dispersion system. On the basis of these topology-controlled PGSs, we establish their topological effect on pigment dispersibility and storage stability. Therefore, this study on pigment dispersion by applying topology-controlled polyethers can demonstrate their potential as synergists in the field of dispersion and further show the topological effect of polymers on dispersibility.

Experimental

Materials

Glycine, 2,3-naphthalenedicarboxylic anhydride, dimethylformamide (DMF) (Sigma-Aldrich; ≥99.8%), ethanolamine (Sigma-Aldrich; ≥99.0%), acrylic acid (Sigma-Aldrich), *N*-(3-dimethylaminopropyl)-*N*′-ethylcarbodiimide hydrochloride (TCI; >98.0%), 4-dimethylaminopyridine (DMA) (TCI; >99.0%), methylene chloride (Sigma-Aldrich, ≥99.8%), 1,8-naphthalic anhydride (TCI; >98.0%), triethylamine (Sigma-Aldrich; ≥99%), benzoyl chloride (Alfa Aesar; 99+%), 1-ethyl-3-(3-dimethylaminopropyl)carbondiimide (EDCI) (TCI; >98.0%), diethyl ether (Burdick & Jackson, ACS), *N*-phthaloylglycine (A_1) (TCI; >98.0%), 9-oxoacridine-10-acetic acid (A_4) (TCI; >98.0%), and anthraquinone-2-carboxylic acid (A_5) (TCI; >99.0%) were used as received without purification. Toluene (Sigma-Aldrich; >99%) was purified by column chromatography prior to use. The molecular sieves (4 Å) were dried at 300 °C using a heating gun under a reduced pressure for 30 min prior to use. Tetralin (Sigma-Aldrich; 99%), tris(pentafluorophenyl)borane ($B(C_6F_5)_3$) (Sigma-Aldrich; 95%), glycidol (Sigma-Aldrich; 96%), and tributylamine (TBA) (Sigma-Aldrich; ≥98.5%) were dried overnight over calcium hydride and purified by distillation. Dimethyl sulfoxide (DMSO, SUNSEI; 99%), 3,4-dihydro-2*H*-pyran (Sigma-Aldrich; 97%), *p*-toluenesulfonic acid (Sigma-Aldrich; ≥98.5%), sodium bicarbonate (DUKSAN; 99%), sodium sulfate, ethyl acetate (Sigma-Aldrich, ≥99.5%), hexane (Sigma-Aldrich; ≥99.5%), phosphazene base P_4-*t*-Bu solution (*t*-BuP_4) (Sigma-Aldrich; ~0.8 M in hexane), benzyl alcohol (Sigma-Aldrich; 99.8%), benzoic acid (Sigma-Aldrich; 99.5%), tetrahydrofuran (THF; ≥99.9%, inhibitor-free), HCl (Sigma-Aldrich, ACS reagent; 37%), MeOH (Sigma-Aldrich; 99%), and potassium carbonate (Sigma-Aldrich, ACS reagent; ≥99.0%) were used as received.

Preparation of topology-controlled poly(glycidol)s (PG)

Branched cyclic (*bc*-PG), hyperbrached (*hb*-PG), and linear polyglycidols (*lin*-PG) were synthesized according to procedures previously reported in the literature.[31,32,35]

General procedure for the preparation of *bc*-PG-BzA_n synergists

The post-polymerization modification of *bc*-PG was performed using syringe technique under dry argon in a baked round-bottom flask equipped with a three-way stopcock. A typical procedure for preparing polymeric synergists using *bc*-PG is described as follows. For example, for *bc*-PG-BzA_1, 4.00 g of *bc*-PG (54.0 mmol for total hydroxyl groups) was placed in a round-bottom flask (250 mL) and completely dissolved in 80 mL of DMF. After the addition of 1.51 mL of triethylamine (11.0 mmol), the mixture was cooled to 0 °C, and 1.26 mL of benzoyl chloride (11.0 mmol) was then slowly added to the mixture. The mixture was stirred at room temperature for 24 h. After the subsequent reaction was completed, 1.04 g of EDCI (5.40 mmol) and 0.330 g of DMAP (2.70 mmol) were introduced to the flask, and 1.11 g of *N*-phthaloylglycine (5.4 mmol) (A_1) was subsequently added. After the completion of the reaction, the solution was precipitated by cold diethyl ether several times to

Table 1 Characterizations of *bc*-PGSs with different anchor groups in this study

Entry	Synergist	M_n[a]	M_w/M_n[a]	T_g[b]	Ratio (–OH/BzCl/anchor)
0	*bc*-PG	1350	2.1	−43	10/0/0
1	*bc*-PG-BzA_1	1070	2.4	−20	7/2/1
2	*bc*-PG-BzA_2	n/d[c]	n/d[c]	−22	7/2/1
3	*bc*-PG-BzA_3	970	2.9	−20	7/2/1
4	*bc*-PG-BzA_4	960	2.7	−11	7/2/1
5	*bc*-PG-BzA_5	870	2.8	−22	7/2/1

[a] The number-averaged molecular weight (M_n) and molecular weight distribution (M_w/M_n) of the synergists were determined by size-exclusion chromatography (SEC) with PEO standard for calibration in DMF. [b] Glass transition temperature (T_g) was analyzed by differential scanning calorimetry (DSC) at a heating rate of 10 °C min^{-1} under nitrogen atmosphere. [c] The molecular weight of *bc*-PG-BzA_2 synergist was not measured because this product was not dissolved in DMF as an eluent used in SEC analysis.

obtain the highly pure product. The resultant *bc*-PG-BzA_1 was vacuum-dried and characterized by size-exclusion chromatography (SEC) (*bc*-PG-BzA_1 in Table 1, $M_n = 1{,}070$, $M_w/M_n = 2.40$).

Synthesis of the *hb*-PG-BzA_1 synergist

The post-polymerization modification of *hb*-PG was performed using syringe technique under dry argon in baked round-bottom flask equipped with a three-way stopcock. A typical procedure for preparing polymeric synergists using *hb*-PG is described as follows. For example, for *hb*-PG-BzA_1, 4.00 g of *hb*-PG (54.0 mmol for total hydroxyl groups) was placed in a round-bottom flask (250 mL) and completely dissolved in 80 mL of DMF. After the addition of 1.51 mL of triethylamine (11.0 mmol), the mixture was cooled to 0 °C, and 1.26 mL of benzoyl chloride (11.0 mmol) was slowly added to the mixture. The mixture was stirred at room temperature for 24 h. After reaction completion, 1.04 g of EDCI (5.40 mmol) and 0.330 g of DMAP (2.70 mmol) were introduced to the flask and 1.11 g of *N*-phthaloylglycine (5.4 mmol) (A_1) was subsequently added. After the subsequent reaction was completed, the solution was precipitated by cold diethyl ether several times to obtain the highly pure product. The resultant *hb*-PG-BzA_1 was vacuum-dried and characterized by SEC (*hb*-PG-BzA_1 in Table S1,† $M_n = 570$, $M_w/M_n = 1.40$).

Synthesis of the *lin*-PG-BzA_1 synergist

The post-polymerization modification of *lin*-PG was performed using syringe technique under dry argon in a baked round-bottom flask equipped with a three-way stopcock. A typical procedure for preparing polymeric synergists using *lin*-PG is described as follows. For example, *lin*-PG-BzA_1, 4.00 g of *lin*-PG (54.0 mmol for total hydroxyl groups) was placed in a round-bottom flask (250 mL) and completely dissolved in 80 mL of DMF. After the addition of 1.51 mL of triethylamine (11.0 mmol), the mixture was cooled to 0 °C, and 1.26 mL of benzoyl chloride (11.0 mmol) was slowly added to the mixture. The mixture was stirred at room temperature for 24 h. After the reaction was completed, 1.04 g of EDCI (5.40 mmol) and 0.330 g of DMAP (2.70 mmol) were introduced to the flask, and 1.11 g of *N*-phthaloylglycine (5.4 mmol) (A_1) was added. After the subsequent reaction was completed, the solution was precipitated by cold diethyl ether several times to obtain the highly pure product. The resultant *lin*-PG-BzA_1 was vacuum-dried and characterized by SEC (*lin*-PG-BzA_1 in Table S1,† $M_n = 600$, $M_w/M_n = 1.50$).

Preparation of pigment dispersions with PG-based synergists under bead milling process

The colorant (pigment dispersion) was prepared following the composition shown in Table S2.† All raw materials at the milling step were charged into the vessel. The mixture was allowed to mix in the high-speed disperser at 2000 rpm to achieve homogeneous dispersion. The pigment dispersion was characterized without further purification.

Evaluation of pigment dispersions

The viscosities of pigment dispersions were analyzed by using Brookfield viscometer (DV-II+Pro) under the condition of 5 rpm for 6 min at 25 °C. To evaluate the storage stability, the dispersion viscosity was analyzed after 5 days at 50 °C of preparing the dispersions and compared with the viscosity of initial sample.

Measurement

The M_n and M_w/M_n of polymers were measured by SEC at 45 °C using DMF as an eluent. For the DMF-SEC, three polystyrene-gel columns [KD-802 (from Shodex); pore size, 150 Å; 8 mm i.d. × 300 mm, KD-803 (from Shodex); pore size, 500 Å; 8 mm i.d. × 300 mm, KD-804 (from Shodex); pore size, 1500 Å; 8 mm i.d. × 300 mm] were connected to a PU-4180 pump, a RI-4030 refractive-index detector, and a UV-4075 ultraviolet detector (JASCO), and the flow rate was set to 1.0 mL min^{-1}. The columns were calibrated against 13 standard poly(ethylene glycol) (PEO) samples (Agilent Technologies; M_p = 980–811 500; M_w/M_n = 1.03–1.11). ^1H NMR was recorded on a Bruker Ultrashield spectrometer operating at 300 MHz. All spectra were recorded in ppm units with deuterated solvents at room temperature. Differential scanning calorimetry (DSC) was conducted on polymer samples under a dry nitrogen flow at a heating or cooling rate of 10 °C min^{-1} on a Q2000 calorimeter (TA Instruments). The viscosities of pigment dispersions were analyzed by using Brookfield viscometer (DV-II+Pro) with CPE-40 spindle. Size analyses were performed using dynamic light scattering (DLS, Zetasizer Nano ZS90, Malvern Instruments).

Results and discussion

Design and synthesis of *bc*-PG based synergists (PGSs)

Numerous synergists have been fabricated with chemically polar moiety or structurally planar molecules because these functional groups facilitate the affinity between dye or pigment and dispersants, leading to the high dispersion and stability in solution. Recently, phthalocyanine derivates modified with functional groups have been reported as a synergists to improve the affinity between pigments and dispersants.[16] Specifically, in anthraquinone derivates, the carbonyl, amine, and hydroxyl groups enable hydrogen bonding with pigment, while the phenoxy group provides affinity with nonpolar bulky hydrocarbons.

To design a synergist having such functionalities, benzoyl chloride was employed as a hydrophobic part with a planar structure, which readily reacted with the hydroxy group in the polymer backbone. In addition, a series of anchoring groups represented by phthalimide, naphthalic imides, acridone, or anthraquinone including carbonyl, amine, or arene groups were individually employed to benzoyl-functionalized PG to improve adhesion performance with red pigment *via* EDCI coupling (Fig. 1).[16] The anchor molecules with naphthalic imides had two types of structures, which were synthesized using naphthalenedicarboxylic anhydride or naphthalic anhydride (see ESI† for Experimental section and Fig. S1†).

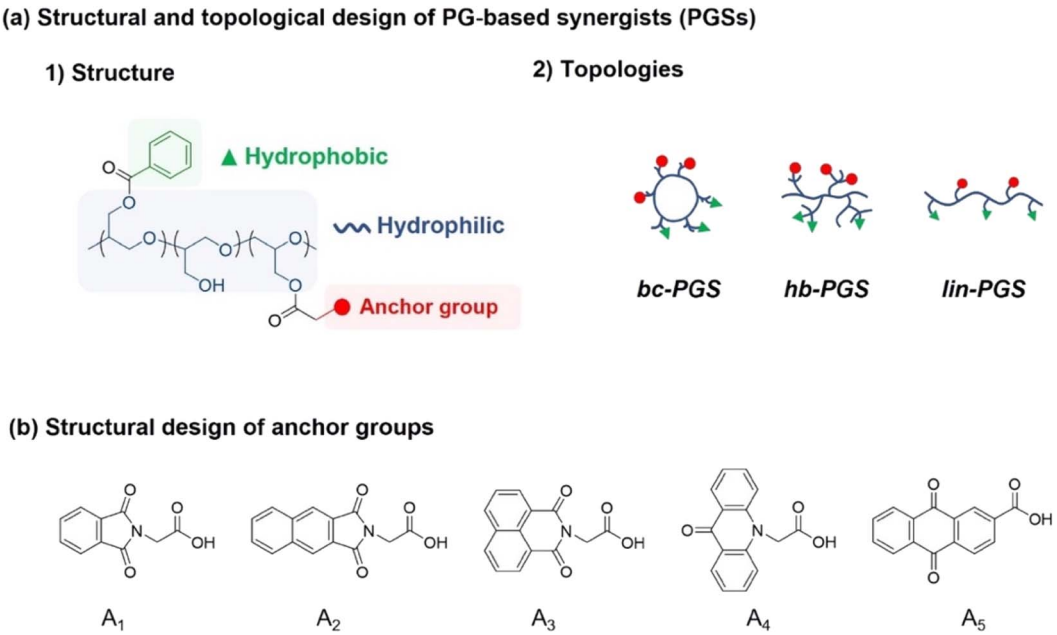

Fig. 1 (a) Design of PG-based synergists (PGSs) with controlled structure and topologies. (b) Design of anchors with functional molecular structures.

To evaluate the effect of various anchor groups on the dispersibility and corresponding stability of dispersions, five polymeric synergists based on the topology-controlled *bc*-PG were first synthesized (Table 1 and Fig. S2†). For example, the aromatic groups from benzoyl and phthalimide groups were clearly confirmed with the peaks in the range of 7.2–8.2 ppm in ^{1}H NMR measurement (Fig. 2). Peak integration between aromatic groups and polymer backbone leads to the ratio of functional groups in synergist, showing 70% of hydroxyl, 20% of benzoyl, and 10% of anchor groups for *bc*-PG-BzA$_1$ (entry 2 in Table 1). In addition, the corresponding relevant molecular weight of obtained product, which was confirmed by SEC analysis, clearly decreased after the reaction owing to the change in hydrodynamic diameter in the solution, and the glass transition temperature (T_g) of *bc*-PG-BzA$_1$ increased T_g possibly because of increased molecular weight and rigid groups from

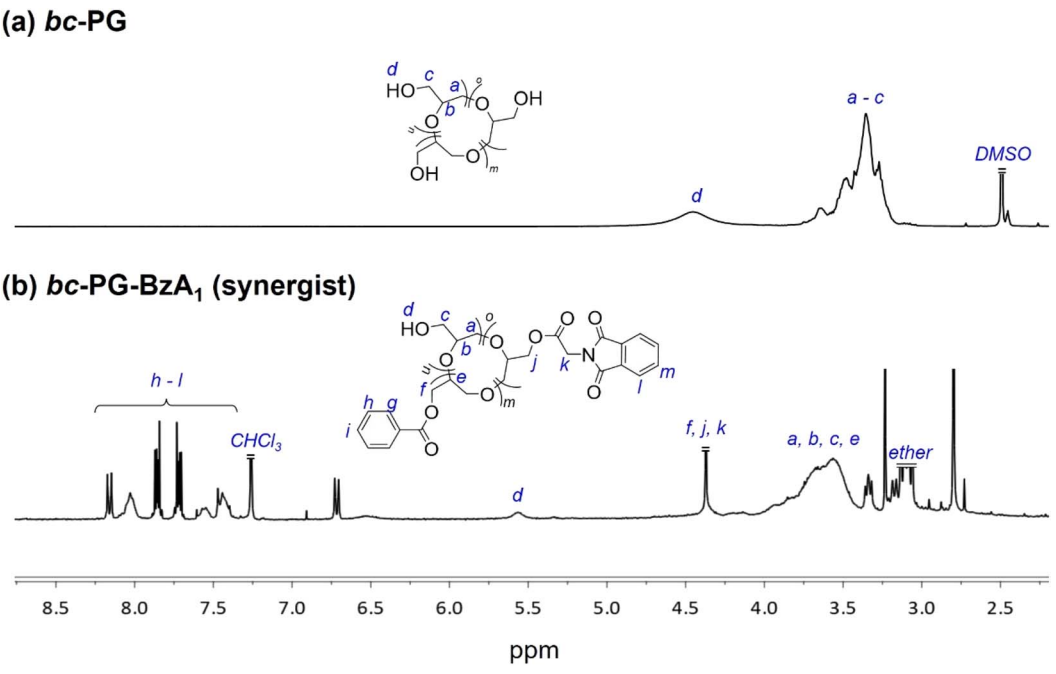

Fig. 2 ^{1}H NMR spectra of (a) *bc*-PG in DMSO and (b) *bc*-PG-BzA$_1$ synergist in $CDCl_3$.

hydrophobic moieties. The characteristics of all samples having similar hydrophobic compositions in the *bc*-PGs in this study are summarized in Table 1.

Effect of synergists on Red 170 dispersions

Red 170 dispersions were prepared through the bead-milling process. To understand the effect of as-prepared synergists on the dispersing performance, the viscosity of Red 170 dispersions, which were formulated with additives such as BYK 190 polymeric dispersant and waterborne *bc*-PG synergists, were monitored at a specific time (Fig. 3 and Table S3†). As a control, in the presence of only the BYK 190 dispersant, the viscosity of the dispersion was optimized under bead-milling process after 12 h, after which an increase in viscosity was observed (square in Fig. 3a). Interestingly, with the addition of imide-type synergists, the optimal bead-milling time was 6 h, which was clearly shorted than that of the control experiment, indicating that these *bc*-PGSs successfully achieved strong adsorption of dispersants on the pigment surface and stabilized the pigment particles at the early dispersion stage. In particular, the red pigment dispersion with *bc*-PG-BzA$_1$ exhibited enhanced dispersion performance of 32% compared to the control at the optimal bead-milling time, indicating relatively excellent dispersibility (red dot in Fig. 3a). These results suggest that the *bc*-PGSs influenced the dispersing performance and that the phthalimide moiety of *bc*-PG-BzA$_1$ synergist had the most efficient interaction with the pigment among the different types of imides for improving the dispersibility of pigment particles. Although *bc*-PG-BzA$_2$ and *bc*-PG-BzA$_3$ showed similar trends as synergists to that of *bc*-PG-BzA$_1$, their increased hydrophobicity in the anchor group might adversely affect the interaction with the pigment in aqueous solutions (blue and pink dots in Fig. 3a).

In addition to the viscosity results, the particle size of the dispersion samples was analyzed to investigate the cohesiveness of the particles in relation to the dispersibility of the pigment solution (Table S3†). Among the four BYK190 dispersion samples prepared with dispersant and synergists, the samples with only a dispersant and those with synergist dispersions containing phthalimide and naphthalene were investigated because of relative potential for improving dispersion performance. The particle of *bc*-PG-BzA$_1$ solution was smaller than that of the BYK 190-only dispersion, indicating that *bc*-PG-BzA$_1$ synergist show superior dispersing performance. Considering that *bc*-PG-BzA$_2$ and *bc*-PG-BzA$_3$, with particle sizes of 320.2 nm and 324.1 nm, respectively, had similar sizes to that of the solution applied with only the dispersant, a well-dispersed pigment solution was formed without flocculation. Nevertheless, the sizes of pigment particles applied with *bc*-PG-BzA$_2$ and *bc*-PG-BzA$_3$ were slightly larger than that of the pigment solution without synergists, thus supporting that *bc*-PG-BzA$_2$ and *bc*-PG-BzA$_3$ used in pigment dispersion had poorer dispersing performance. Based on the results from viscosity and DLS analyses, the *bc*-PG-BzA$_1$ with phthalimide moiety could be potentially utilized as the optimal synergist to achieve a high dispersion performance in the BYK 190 system.

Meanwhile, the *bc*-PG-BzA$_4$ and *bc*-PG-BzA$_5$ synergists tend to increase the viscosity by milling (Fig. 3b). For example, the *bc*-PG-BzA$_4$ and *bc*-PG-BzA$_5$, which had the acridone and anthraquinone groups, respectively, showed 35.9 and 149.2 cps point increases, respectively (Table S3†). These results indicate that *bc*-PG-BzA$_4$ synergist with acridone molecule is relatively advantageous as a synergist to improve dispersibility. However, because the dispersion viscosity with both synergists was increased through ball milling, improving dispersibility by applying these synergists is difficult.

Colloid stability is the most important property in pigment dispersion solutions. Poor dispersion stability can lead to coagulation or agglomeration, increase in size and viscosity, aggregation and precipitation, and phase separation or gelation.[36–38] Additives such as dispersants and synergists should improve the dispersion of pigment solutions, as well as provide long-term storage stability without disturbing solution

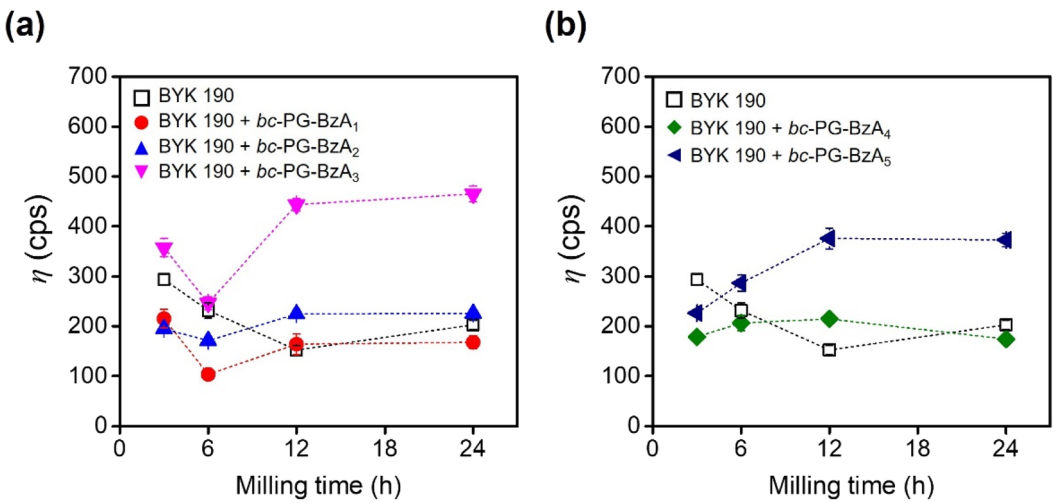

Fig. 3 Viscosities of Red 170 dispersion formulated with BYK 190 dispersant and a series of *bc*-PG synergists as a function of milling time.

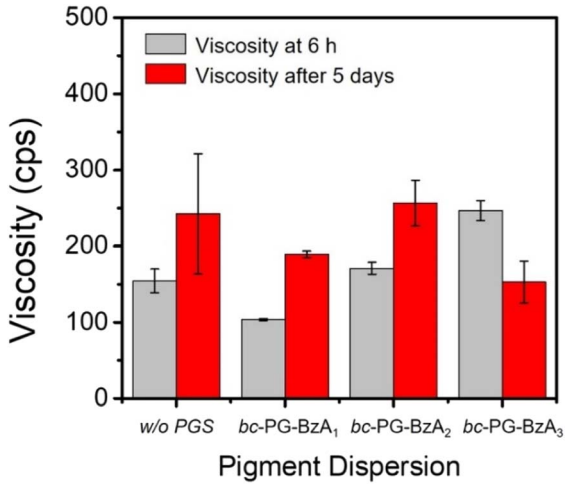

Fig. 4 Storage stability of Red 170 dispersions in *bc*-PG synergist systems.

stability. To evaluate the storage stability of the pigment dispersion solutions, we investigated the solution viscosity and particle size in solution after storage at 50 °C for 5 days (Fig. 4 and Table S4†). For example, for entry 1 in Table S4,† that is, the dispersion using BYK 190 without synergist, viscosity and particle size increased by 88.0 cps and 28.8 nm, respectively, after storage owing to the coagulation. Although the dispersions using BYK 190 and *bc*-PG-BzA_1 showed similar increases to those of the control, the change in particle size was relatively smaller than that of the dispersion using BYK 190. In particular, the low standard deviation for viscosity of the dispersion using BYK 190 and *bc*-PG-BzA_1 indicates uniform particles and a relatively stable solution state in the long-term storage at high temperature. By contrast, the decreased viscosity of *bc*-PG-BzA_3 in Fig. 4 was attributed to particle agglomeration, causing precipitation or gelation and indicating low storage stability. Nevertheless, most of the prepared pigment dispersions showed proper stability under severe conditions. These results support that the *bc*-PGS influence the stability of the dispersion as well as the dispersibility.

Topology-controlled polymeric synergists in dispersion

Based on the results of dispersant- or synergist-based pigment dispersion experiments, *bc*-PG modified with benzoyl and anchor groups are suitable in pigment dispersion systems. In particular, among anchor molecules, the phthalimide structure was demonstrated to be useful as a synergist for pigment dispersion. Given the excellent dispersing performance of the combination of BYK 190 and *bc*-PG-BzA_1, the phthalimide and benzoyl moieties were employed in topology-controlled PGs (linear and hyperbranched PGs). The topology-controlled synergists were similarly synthesized and analyzed in the same manner as *bc*-PG-BzA_1 (Fig. S3†).

To investigate the effect of polymer topologies on the dispersion system, topology-controlled *hb*-PGS and *lin*-PGS were employed in the dispersion formulation, which was identical to that of the *bc*-PG-BzA_1 system. Therefore, each viscosity change of dispersions was first monitored to optimize the bead-milling time (Fig. 5a). Similarly, the optimal bead-milling time for each case was 6 h, which was identical to that of the *bc*-PGS system, indicating that the topology-controlled *hb*-PGS and *lin*-PGS successfully achieved a strong adsorption of dispersants on the pigment surface and were stabilized (Fig. 5a). However, the *lin*-PG-BzA_1 synergist system was more viscous than the others, supporting that the branched polymer structures, *bc*-PG-BzA_1 and *hb*-PG-BzA_1, which had steric conformance, exhibited better binding ability with pigment particles and dispersants than the linear analog. Zeng *et al.* reported that branched polyurethane dispersants exhibited outstanding dispersing property because of their three-dimensional structure and numerous functional groups. In particular, the structure of the branch of the polymer dispersant adsorbed on the surface of the pigment particle formed a steric hindrance to prevent the aggregation of the pigment particle, thereby ensuring dispersion stability.[11] In addition, because the *lin*-PG-BzA_1 system had higher viscosity

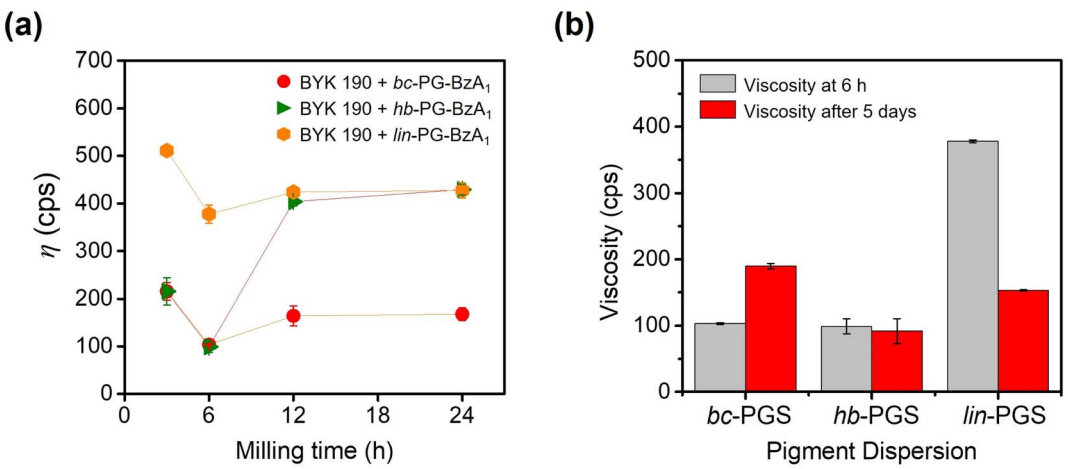

Fig. 5 (a) Viscosities of Red 170 dispersion depending on topology-controlled PG synergists and (b) long-term stability of pigment dispersion with BYK 190 depending on the topology-controlled PGSs after storage for 5 days at 50 °C.

than that with only the BYK 190 dispersant, the use of *lin*-PG-BzA_1 as a synergist eventually disturbed the dispersing performance in the pigment solution.

To understand the effect of polymer topologies on the storage stability in the dispersion, we analyzed the changes in the viscosity and particle sizes of each pigment solution stored at 50 °C for 5 days (Fig. 5b and Table S5†). While the *bc*-PG-BzA_1 provided relatively good high-temperature storage stability, *hb*-PG-BzA_1 showed excellent high-temperature storage stability. For example, in contrast to that using *bc*-PG-BzA_1, the viscosity of dispersion using *hb*-PG-BzA_1 was 91.9 cps after 5 days of storage, which was similar to the viscosity of the system before storage. In addition, the coagulation behavior of dispersed particles was not induced during high-temperature storage. Coagulation did not occur because the steric hindrance on the surface of pigment by hyperbranched structure of *hb*-PG-BzA_1 prevented the flocculation of pigment particles during storage.[11,26] However, the *lin*-PG-BzA_1 system showed a decrease in viscosity of dispersion to 152.9 cps from the initial 378.0 cps, and the particle size was reversibly increased to 352.2 nm. This finding demonstrated that such a linear structure had low dispersing ability in the initial dispersion and was not effective for preventing particle aggregation by flocculation during long-term storage.[39,40] Therefore, the *lin*-PG-BzA_1 dispersion system was not suitable for improving the dispersibility and stability of pigment solution.

Conclusions

This study successfully synthesized *bc*-PG-based waterborne synergists with different anchor groups through simple post-polymerization modification and employed to a Red 170 dispersion system with BYK 190 as polymeric dispersant. Particularly, the phthalimide group as an anchor group enhanced the performance of the Red 170 dispersion system and was identically applied to the *hb*-PG and *lin*-PG to evaluate the effect of polymer topologies. Although these three types of waterborne synergists improved the dispersion performance, branched type PGSs were the most effective for enhancing the Red 170 dispersibility because they achieved strong adsorption of dispersants on the pigment surface and stabilized the pigment particles at the early dispersion stage. Despite similar structural features between *bc*-PGS and *hb*-PGS, interestingly, *hb*-PGS promoted stable storage stability at high temperatures through steric hindrance on the surface of the pigment particles. Therefore, we expect that this new approach on the topological effects of polymeric synergists for the pigment dispersion to contribute to the development of advanced waterborne synergists with considerable potential for dispersion systems.

Author contributions

The manuscript was written with contributions from all authors. All of the authors approved the final version of the manuscript. H. K. and S. E. K.: experimentation, analysis, and writing; Y. I. P., J. C. K, J.-E. J., H. J., H. L: analysis; S. Y. H., I. W. C., S.-H. L., and E. S.: conceptualization, supervision, and editing.

Conflicts of interest

The authors declare no competing financial interest.

Acknowledgements

This study was supported by the Ministry of Trade, Industry and Energy (MOTIE, Korea) under the Industrial Technology Innovation Program (No. 20011123) and the Korea Research Institute of Chemical Technology (KRICT) (No. KS2341-20). This work was supported by the National Research Foundation of Korea (NRF) grant funded by the Korean government (MSIT) (RS-2022-00165897). This work was also supported by the Ministry of Science, ICT & Future Planning (NRF-2022M3J4A1091450).

References

1 T. Masuda, Y. Kudo and D. Banerjee, *Coatings*, 2018, **8**, 282.
2 S. Singh, S. K. Pandey and N. Vishwakarma, in *Handbook of functionalized nanomaterials for industrial applications*, Elsevier, 2020, pp. 717–730.
3 G. Carotenuto, Y. S. Her and E. Matijevic, *Ind. Eng. Chem. Res.*, 1996, **35**, 2929–2932.
4 A. G. Abel, *Paint and Surface Coatings: Theory and Practice*, 1999, pp. 91–165.
5 E. Baez, N. Quazi, I. Ivanov and S. N. Bhattacharya, *Adv. Powder Technol.*, 2009, **20**, 267–272.
6 A. Gürses, M. Açıkyıldız, K. Güneş and M. S. Gürses, *Dyes Pigm.*, 2016, 13–29.
7 H. Widiyandari, F. Iskandar, N. Hagura and K. Okuyama, *J. Appl. Polym. Sci.*, 2008, **108**, 1288–1297.
8 H. J. Spinelli, *Adv. Mater.*, 1998, **10**, 1215–1218.
9 Z. Pu, X. Fan, J. Su, M. Zhu and Z. Jiang, *Colloid Polym. Sci.*, 2022, **300**, 167–176.
10 C. Auschra, E. Eckstein, A. Muhlebach, M. O. Zink and F. Rime, *Prog. Org. Coat.*, 2002, **45**, 83–93.
11 T. Zeng, G. He, X. Li and C. Wang, *J. Appl. Polym. Sci.*, 2021, **138**, 50790.
12 J. Choi, W. Lee, J. W. Namgoong, T. M. Kim and J. P. Kim, *Dyes Pigm.*, 2013, **99**, 357–365.
13 F. O. H. Pirrung, P. H. Quednau and C. Auschra, *Chimia*, 2002, **56**, 170–176.
14 C. Agbo, W. Jakpa, B. Sarkodie, A. Boakye and S. H. Fu, *J. Dispersion Sci. Technol.*, 2018, **39**, 874–889.
15 M. M. Gacek and J. C. Berg, *Electrophoresis*, 2014, **35**, 1766–1772.
16 J. W. Namgoong, S. W. Chung, H. Jang, Y. H. Kim, M. S. Kwak and J. P. Kim, *J. Ind. Eng. Chem.*, 2018, **58**, 266–277.
17 C. Yoon, J. H. Choi and J. P. Kim, *Mol. Cryst. Liq. Cryst.*, 2010, **533**, 102–112.

18 A. T. Kelley, P. J. Alessi, J. E. Fornalik, J. R. Minter, P. G. Bessey, J. C. Garno and T. L. Royster, *ACS Appl. Mater. Interfaces*, 2010, **2**, 61–68.
19 C. Yoon and J. H. Choi, *Dyes Pigm.*, 2014, **101**, 344–350.
20 G. Nian, J. Kim, X. Bao and Z. Suo, *Adv. Mater.*, 2022, **34**, e2206577.
21 T. Liu, W. Chen, K. Li, S. Long, X. Li and Y. Huang, *Polymers*, 2023, **15**, 2644.
22 B. I. Voit and A. Lederer, *Chem. Rev.*, 2009, **109**, 5924–5973.
23 R. A. Shenoi, J. K. Narayanannair, J. L. Hamilton, B. F. Lai, S. Horte, R. K. Kainthan, J. P. Varghese, K. G. Rajeev, M. Manoharan and J. N. Kizhakkedathu, *J. Am. Chem. Soc.*, 2012, **134**, 14945–14957.
24 C. J. Hawker and J. M. J. Frechet, *J. Am. Chem. Soc.*, 1990, **112**, 7638–7647.
25 S. Y. Lee, M. Kim, T. K. Won, S. H. Back, Y. Hong, B. S. Kim and D. J. Ahn, *Nat. Commun.*, 2022, **13**, 6532.
26 D. J. Lunn, S. Seo, S. H. Lee, R. B. Zerdan, K. M. Mattson, N. J. Treat, A. J. McGrath, W. R. Gutekunst, J. Lawrence, A. Allison, A. Anastasaki, A. S. Knight, B. V. K. J. Schmidt, M. W. ates, P. G. Clark, J. P. DeRocher, A. K. Van Dyk and C. J. Hawker, *J. Polym. Sci., Part A: Polym. Chem.*, 2019, **57**, 716–725.
27 T. P. Holbrook, G. M. Masson and R. F. Storey, *J. Polym. Sci., Part A: Polym. Chem.*, 2019, **57**, 1682–1696.
28 G. Y. Wang, Y. Y. Bai, X. Y. Ma, W. X. Wang, Q. W. Yin and Z. P. Du, *J. Mol. Liq.*, 2017, **225**, 333–338.
29 G. P. Lokhande and R. N. Jagtap, *Prog. Org. Coat.*, 2016, **90**, 359–368.
30 Y. Y. Xu, J. C. Liu, C. S. Du, S. H. Fu and X. Y. Liu, *Prog. Org. Coat.*, 2012, **75**, 537–542.
31 S. E. Kim, H. J. Yang, S. Choi, E. Hwang, M. Kim, H.-J. Paik, J.-E. Jeong, Y. I. Park, J. C. Kim, B.-S. Kim and S.-H. Lee, *Green Chem.*, 2022, **24**, 251–258.
32 S. E. Kim, Y. R. Lee, M. Kim, E. Seo, H. J. Paik, J. C. Kim, J. E. Jeong, Y. I. Park, B. S. Kim and S. H. Lee, *Poly. Chem.*, 2022, **13**, 1243–1252.
33 J. Kim, S. Choi, J. Baek, Y. I. Park, J. C. Kim, J. E. Jeong, H. Jung, T. H. Kwon, B. S. Kim and S. H. Lee, *Adv. Funct. Mater.*, 2023, 2302086.
34 S. Choi, J. Kim, E. Seo, H. Y. C. Jung, J. E. Jeong, Y. I. Park, J. C. Kim, D. W. Lee, B. S. Kim and S. H. Lee, *Poly. Chem.*, 2023, **14**, 1184–1194.
35 J. Song, L. Palanikumar, Y. Choi, I. Kim, T. Y. Heo, E. Ahn, S. H. Choi, E. Lee, Y. Shibasaki, J. H. Ryu and B. S. Kim, *Poly. Chem.*, 2017, **8**, 7119–7132.
36 J. Dong, S. Chen, D. S. Corti, E. I. Franses, Y. Zhao, H. T. Ng and E. Hanson, *J. Colloid Interface Sci.*, 2011, **362**, 33–41.
37 E. S. Fabjan, M. Otonicar, M. Gaberscek and A. S. Skapin, *Dyes Pigm.*, 2016, **127**, 100–109.
38 C. C. Li, S. J. Chang, C. W. Wu, C. W. Chang and R. H. Yu, *J. Colloid Interface Sci.*, 2017, **506**, 180–187.
39 Y. Wang, J. E. Q. Quinsaat, T. Ono, M. Maeki, M. Tokeshi, T. Isono, K. Tajima, T. Satoh, S. I. Sato, Y. Miura and T. Yamamoto, *Nat. Commun.*, 2020, **11**, 6089.
40 M. A. Aboudzadeh, J. Kruse, M. Sanroman Iglesias, D. Cangialosi, A. Alegria, M. Grzelczak and F. Barroso-Bujans, *Soft Matter*, 2021, **17**, 7792–7801.